ACS OMEGA

Article

Cite This: ACS Omega 2019, 4, 18677−18684

http://pubs.acs.org/journal/acsodf

Michael-Type Addition of Gelatin on Electrospun Nanofibrils for Self-Assembly of Cell Sheets Composed of Human Dermal Fibroblasts

Ju Won Lee[†] and Hyuk Sang Yoo*[,†,‡]

[†]Department of Biomedical Materials Engineering and [‡]Institute of Bioscience and Biotechnology, Kangwon National University, Chuncheon 24341, Republic of Korea

Supporting Information

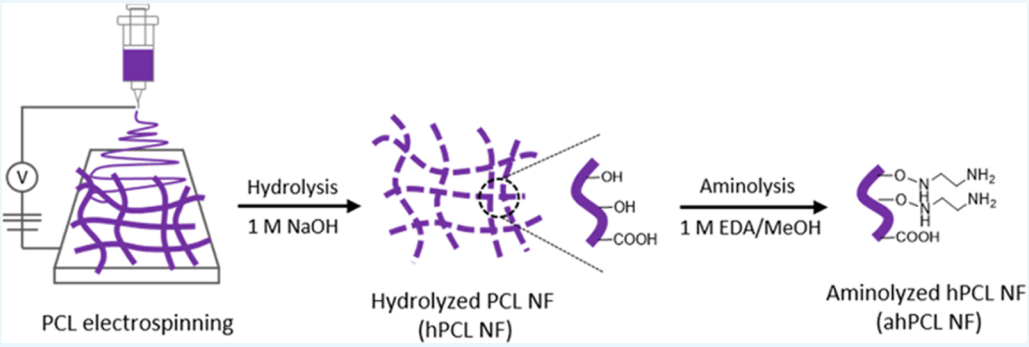

ABSTRACT: To facilitate cell sheet formation of human dermal fibroblasts, gelatin moieties were chemically decorated onto the surface of electrospun nanofibrils (NFs). Poly(caprolactone) [PCL] was electrospun onto fibrous meshes and then fragmented into nanofibrils by optimized milling and hydrolysis. After aminolysis of the NFs, methacrylated gelatin (GelMA) was reacted via Michael-type addition with the surface-exposed amines of the aminolyzed NFs (ahPCL NFs). GelMA was immobilized on the ahPCL NFs. Analysis of ahPCL NFs and native NFs conducted using X-ray photoelectron spectroscopy confirmed that gelatin was chemically conjugated onto the NFs. Human dermal fibroblasts (HDF) and the decorated NFs were self-assembled into cell sheets, and cells in the matrix showed highly spreading morphology by confocal microscopy. Our results indicate that the degree of cell spreading and cellular viability was much higher in the presence of GelMA immobilized in ahPCL NFs.

INTRODUCTION

Three-dimensional (3D) cell culture has recently been used in cell sheet engineering, drug discovery, and cell-based biosensor development because cells in a 3D culture system show behaviors similar to those shown by cells in living organisms.[1−4] The development of 3D culture methods to replace two-dimensional cell culture on film surfaces has been a major goal in the research community.[5] These methods include the use of scaffolds, hydrogels,[6−8] electrospinning,[9−12] and temperature-sensitive polymers.[13,14]

The advantages of electrospinning include straightforward implementation, conditions similar to those of an extracellular matrix (ECM), a high surface-area-to-volume ratio, topographical cues, a rapid exchange of nutrients and waste, and low inflammatory response upon implantation.[15−17] In hydrogels, cells exhibit a round appearance and do not stretch. In nanofibers that possess topographic features, cells are stretched and show proliferative behavior.[18] Similarly, fibroblasts in hydrogels do not behave properly and assume a round shape, but actin stretches effectively in a composite containing nanofibrils (NFs). Hydrogels containing a higher content of NFs result in more distinct topographic effects on cells grown in these scaffolds. The higher the content, the greater the effect due to their topographic effect on cells in hydrogels.[19] In a previous study, we used coaxial electrospinning to synthesize hydrophilic PCL/AL@NF containing hydrophobic polymer poly(caprolactone) (PCL) and hydrophilic alginate (AL) in the outer layer and core, respectively, which allows two immiscible solvents to be electrospun.[20] In this reaction, the calcium bridge in alginate was dependent on the concentration of calcium in the solution. Topographic features of the nanofibers become distinct at high temperatures, and our results showed increased cellular infiltration. Moreover, because cell infiltration is difficult to allow in dense nanofibers,[21] in the present study, we fragmented our NFs via hydrolysis.[22]

Hydrophobic polymers are used to produce nanofibers in conventional electrospinning. This is because electrospinning

Received: August 13, 2019
Accepted: October 15, 2019
Published: November 1, 2019

DOI: 10.1021/acsomega.9b02602
ACS Omega 2019, 4, 18677−18684

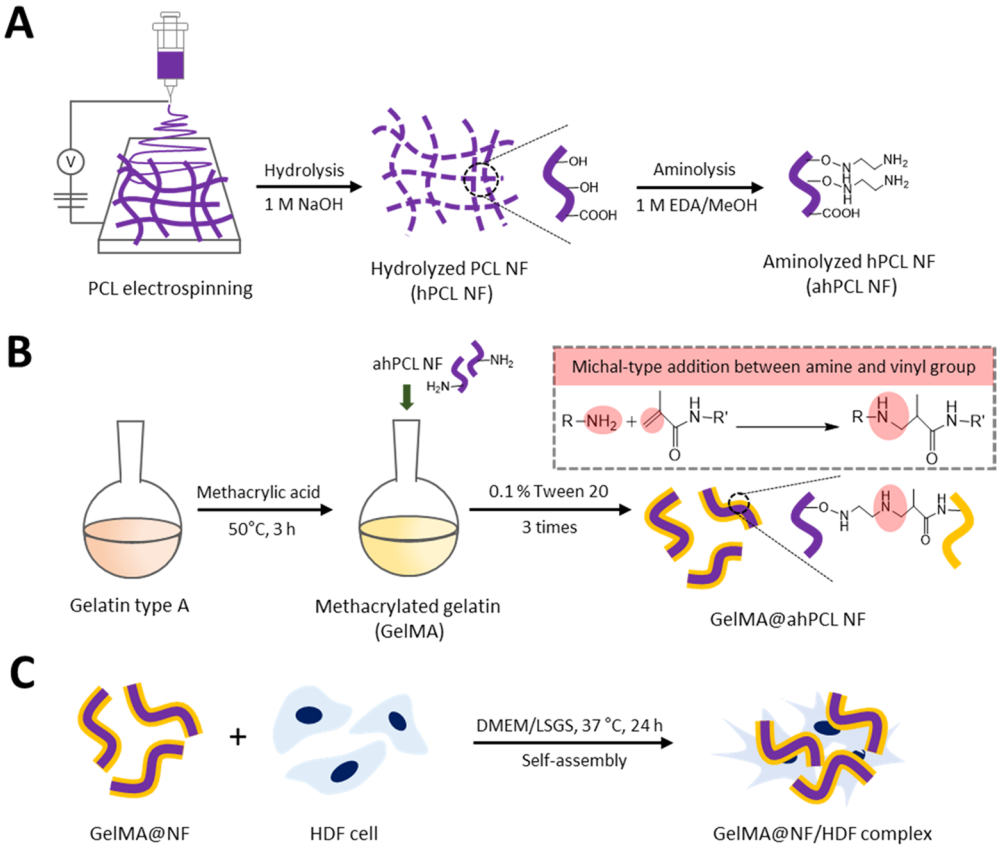

Figure 1. Scheme of the GelMA-immobilized aminolyzed hPCL nanofibrils (ahPCL NFs) for cell adhesion and proliferation. (A) Electrospun PCL fibers were hydrolyzed with sodium hydroxide to make fibrils and aminolyzed by ethylendiamine to substitute amine groups. (B) Synthesis of methacrylic gelatin (GelMA) and chemical reaction with GelMA on the NF surface through Michael-type addition. (C) GelMA@ahPCL NF enhanced the cell proliferation and stretching.

using an organic solvent is more advantageous than using an aqueous phase for obtaining polymerization. Among these, polyesters, such as polylactic acid (PLA)−polyglycolic acid (PGA) and poly(caprolactone) (PCL), have been used extensively in fibrous meshes because these polymers possess excellent biocompatibility and processing properties and are biodegradable.[23−25] However, these materials do not swell, and are hydrophobic and rigid, which limits cell migration and proliferation. To overcome these issues, we previously prepared fragmented electrospun PCL nanofibers and surface-decorated the matrix with cationic and hydrophilic polymeric brushes to sequester multiple proteins.[22] The adsorbed proteins in the decorated matrix exerted bioactive effects, which does not occur in a nondecorated matrix. With an aim to decorate the nanofiber with hydrophilic polymers, we also prepared electrospun nanofibers composed of a PCL−poly(ethyleneimine) (PEI) copolymer and PEG chains were chemically conjugated to the surface-exposed amines.[26] However, the surface density of the amines were relatively low, which caused insufficient decoration of PEG on the surfaces.

Several studies have shown that aminolysis reduces synthesis complexity and increases the number of topographical cues on the film surface. Deschrevel et al. used atomic force microscope to show that roughness of a PLA film surface increases with increasing concentration of 1,6-hexanediamine solution, or with duration of aminolysis.[27] Aminolysis removes the ester bonds present in polyester and exposes the amine groups on polyester surface as amide bonds are formed.[28] Various biomolecules have been used to alter the properties of polymer surfaces. The widely used gelatin contains a peptide related to cell adhesion (arginine−glycine−aspartic acid), which affects cellular migration, proliferation, and differentiation. However, the structural stability of gelatin-containing scaffolds is limited because gelatin dissolves in water at 37 °C, which is the temperature of the human body. Methacrylated gelatin (GelMA) is produced by treating gelatin with methacrylic anhydride; this can change the hardness of a hydrogel by shortening the time needed for UV exposure.[29] We have recently demonstrated that cellular proliferation and differentiation can be increased considerably using NFs. This approach eliminates the need for a collagen matrix and allows for the culture of fibroblast and epithelial cell lines.[30] The Michael-type addition is a nucleophilic addition of a carbanion or another nucleophile to an α,β-unsaturated carbonyl compound. This reaction is traditionally used in materials science to prepare hydrogels,[31,32] polymer films,[33] and gold nanoparticles.[34] When the thiol group of poly(ethylene glycol) hexathiol is mixed with the acrylate group of poly(ethylene glycol) tetraacrylate at a 1:1 ratio, the poly(ethylene glycol)-(PEG)-based hydrogel was synthesized within 10 min.[35] Disadvantages of using a thiol-Michael-type addition include malodorous precursors that contain thiol groups and the possible degeneration of the disulfide, which occurs because of the thiol groups and a lack of spatial and temporal control of the network structure during gelation.[36] To address these issues, Lensen et al. produced a hydrogel via an amine Michael-type addition.[31] An eight-arm poly(ethylene glycol) acrylate

DOI: 10.1021/acsomega.9b02602
ACS Omega 2019, 4, 18677−18684

Table 1. Surface-Decorated Gelatin Moieties on NFs[a]

NF	amount of NF (mg)	initial concentration of gelatin equivalent (μg/mL)	gelatin		GelMA	
			amount of attached gelatin (μg)	incorporation efficiency (%)[b]	amount of attached gelatin (μg)	incorporation efficiency (%)[b]
hPCL NF	1	1	2.14 ± 0.36	2.14 ± 0.36	2.14 ± 0.36	2.14 ± 0.36
		100	9.29 ± 3.73	9.3 ± 3.70	19.21 ± 2.35	19.2 ± 2.40
ahPCL NF		1	3.10 ± 1.03	30.1 ± 10.3	4.76 ± 0.24	46.2 ± 2.40
		100	9.64 ± 1.24	9.6 ± 1.20	10.40 ± 2.00	10.4 ± 2.00

[a]The attached amount of native gelatin or GelMA on NF (6 h) was quantified by directly measuring protein amounts in dissolved PCL NF with a BCA-based protein assay kit. [b]Incorporation efficiency (%) = $(G_t/G_i) \times 100$, where G_t is the amount of attached gelatin that was incubated for 6 h and G_i is the amount of gelatin initially added.

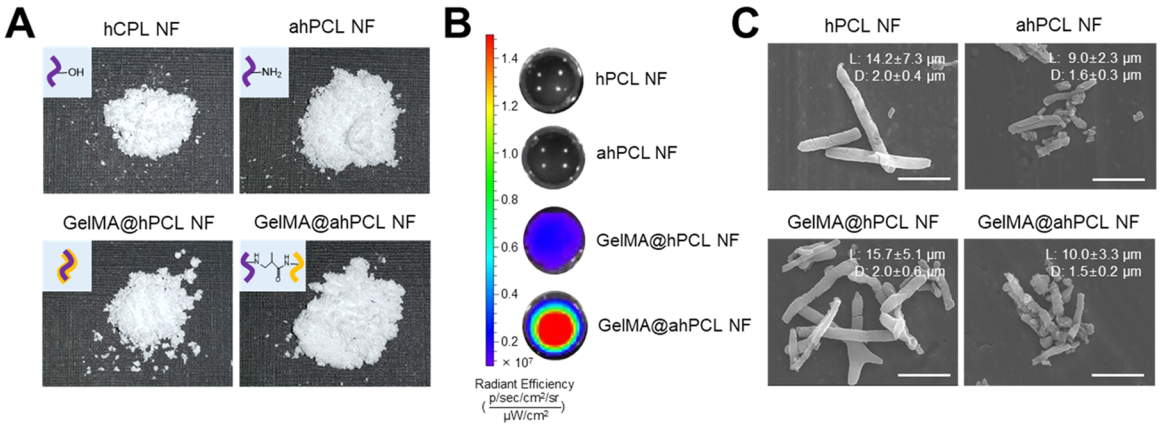

Figure 2. Characterization of GelMA-immobilized ahPCL NF. (A) Digital image of NF (10 mg), (B) in vivo fluorescence image of nanofibrils (NFs) decorated with FITC-labeled GelMA by IVIS, and (C) field-emission scanning electron microscopy (FE-SEM) images of hPCL NF, ahPCL NF, GelMA@hPCL, and GelMA @ahPCL NF. Scale bar = 10 μm and measurement of the length and diameter for NFs using ImageJ.

(8PEG) hydrogel was formed via the Michael-type reaction using 8PEG and 8PEG-NH_2. As the ratio of NH_2 in the polymer increased, the time needed for gelation decreased from a maximum of 170 min to less than 5 min. This 3D culture system used various chemical modifications on the matrix surface to more accurately mimic the conditions of living tissues, thereby increasing cellular affinity for this matrix.

In this study, we developed a straightforward approach for fragmentizing electrospun fibers used to modify the surfaces of NFs affixed to GelMA via Michael-type addition. Because gelatin moieties can be easily decorated on the surface of the nanofiber by a simple chemistry, gelatin-based nanofibrils can affect proliferation and differentiation of cultivating cells to form a cell/matrix assembly.

RESULTS AND DISCUSSION

In this study, we used a straightforward method to fragmentize electrospun fibers and modify the surfaces of NFs that had been affixed to GelMA by chemical bonding via Michael-type addition. During the coculture of cells and NFs, the cells and fragmented fibers spontaneously formed cell sheets. Using these cell sheets, we then evaluated the effects of PCL-based scaffolds on cell proliferation, adhesion, and spreading (Figure 1). The fibers were initially prepared using biodegradable PCL by electrospinning. We then fragmentized the fibers into hydrolyzed nanofibrils (hPCL NFs) so that hydroxyl groups are exposed on the surface. Surface-exposed amine groups were generated by treating NFs with ethylenediamine via aminolysis (ahPCL NFs) (Figure 1A). This simple method improves the hydrophilicity of polymer surfaces and cytocompatibility.[37] Furthermore, this reaction also roughens the surface down to the depth of several micrometers.[38] In our previous study, we used PEI moieties to functionalize the surface of a nanofiber with primary amines.[26] We first synthesized carboxyl-terminated PCL by ring-opening polymerization of ε-caprolactone and octanoic acid and then chemically conjugated PEI to the carboxyl end of PCL to generate a PCL−PEI block copolymer. However, the block copolymer was highly hydrophobic and needed to be modified to increase hydrophilicity. Increasing hydrophilicity is a prerequisite for improving proliferation. Thereby, we electrospun the copolymers and then multilayered PEG on the copolymer mat surface after activating the hydroxyl groups on PEG. To increase the hydrophilicity of the PCL−PEI mesh, we conjugated PEG onto the surface of the mesh and used ahPCL NFs to further modify the matrix surface and to enhance the hydrophilic properties of NFs. However, we developed a simpler method for decorating the polymer surface with primary amines for enhanced functionalization. The amount of primary amine groups in the ahPCL NFs was 355 ± 29.3 nmol/mg using fluorescamine assay. In comparison to our previous study of PCL-PEI block copolymer, it was 58.34 ± 10.04 nmol/mg of amines on it. As shown in Figure 1B, we first reacted ahPCL NF and the methacrylate group of GelMA with an amine group via Michael addition without any further activation of the polymers. Then, we chemically conjugated GelMA onto NFs. We previously showed that PCL NFs can spontaneously associate with cells in culture to form cell/matrix complexes. In the present study, we cultivated GelMA NFs with human dermal fibroblasts (HDF) and evaluated how NFs decorated with GelMA affect the formation of cell sheets, as well as cell spreading and proliferation (Figure 1C).

DOI: 10.1021/acsomega.9b02602
ACS Omega 2019, 4, 18677−18684

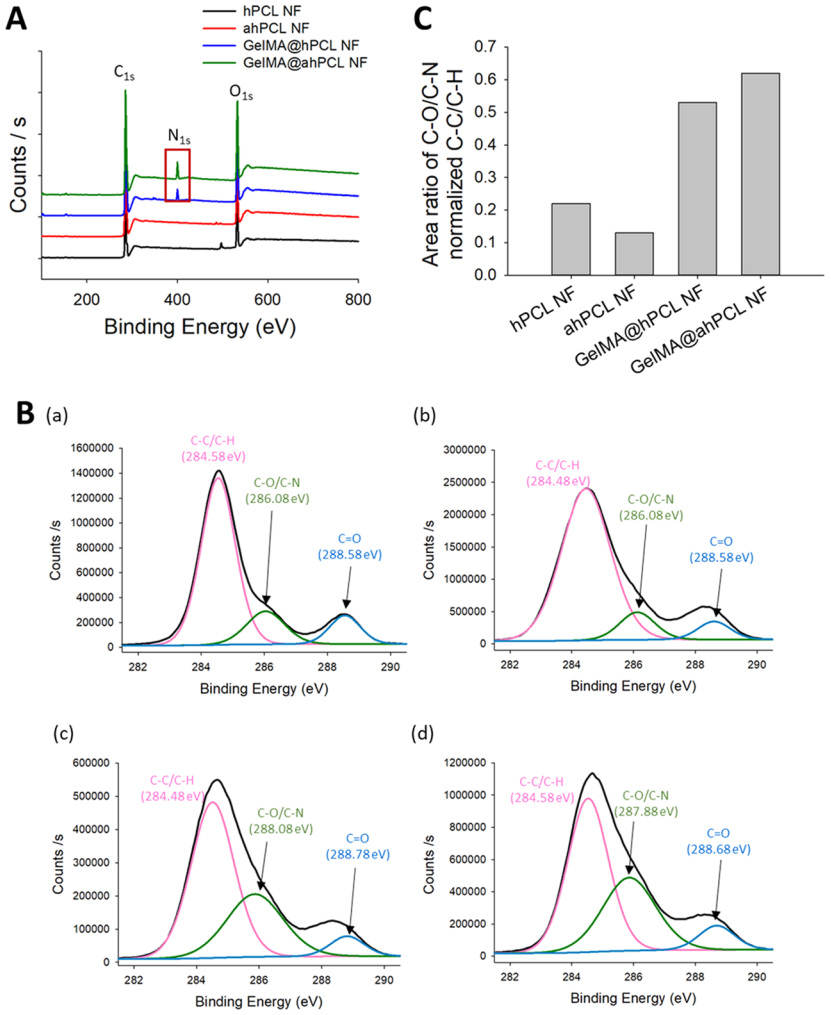

Figure 3. Surface characterization of GelMA-decorated ahPCL NF. (A) XPS spectra of C 1s, N 1s, and O 1s for hPCL NF (black), ahPCL NF (red), GelMA@hPCL NF (blue), and GelMA@ahPCL NF (green). (B) High-resolution XPS spectra for C 1s peaks for (a) hPCL NF, (b) ahPCL NF, (c) GelMA@hPCL NF, and (d) GelMA@ahPCL NF. (C) Area ratio of XPS of carbon atom-linked molecules in NFs.

To evaluate the effects of GelMA on NF, we incubated gelatin or GelMA with hPCL or ahPCL NF at different concentrations. The amount of proteins attached to each NF was measured by directly quantifying the amount of protein incorporated in gelatin and that of GelMA incorporated in NF by melting the protein-containing NFs in hot water (Table 1). We found that at low concentrations of protein used for incorporation (1 μg/mL gelatin equivalent), GelMA@ahPCL showed the highest level of protein incorporation compared with that of GelMA@hPCL, gelatin@ahPCL, and gelatin@hPCL. However, no differences between the complexes were found when a higher concentration of gelatin equivalent was employed for surface decoration (100 μg/mL gelatin equivalent). We speculate that the surface-exposed amines on ahPCL contributed to a higher degree of protein incorporation via Michael-type addition by methacrylate groups of GelMA and surface-amine groups. However, an excessive concentration of protein may induce protein−protein aggregation rather than Michael-type reactions between amines and methacrylates. Thus, the Michael-type reaction can be advantageous when low concentrations of protein are employed for surface decoration on ahPCL NFs.

Digital images were used to evaluate the overall morphology of individual NFs and to compare volumetric differences during the preparation of GelMA@ahPCL NFs (Figure 2A). Using the same weight of freeze-dried NFs (10 mg), GelMA@ahPCL NF exhibited the highest volume, which is followed by those of ahPCL and GelMA@hPCL. GelMA@ahPCL NFs showed "fluffy" morphology upon freeze-drying, which increased the mass of these NFs. We speculate that these differences are caused by surface-charge upon aminolysis. ahPCL NFs exhibited higher amine density on the surface, indicating that electrostatic repulsion among NFs can be increased in functionalized NFs compared with that of non-treated NF. To evaluate the degree of attachment between GelMA and ahPCL NFs, various NFs were incubated with fluorescently stained GelMA for 1 h and the fluorescence intensity was determined by in vivo imaging system (IVIS) (Figure 2B). To eliminate non-covalently associated protein from the NFs, protein-bound NFs were washed thrice with Tween-20. hPCL NFs, and ahPCL NFs without GelMA did not emit fluorescence. However, GelMA@ahPCL NFs containing the amine groups on their surface (added via chemical reaction) emitted a higher fluorescence intensity than that of GelMA@hPCL NFs (containing GelMA added via physical coating). These findings indicate that a greater amount of GelMA was fixed on ahPCL NFs than that on hPCL NFs, showing that Michael-type chemical addition

DOI: 10.1021/acsomega.9b02602
ACS Omega 2019, 4, 18677−18684

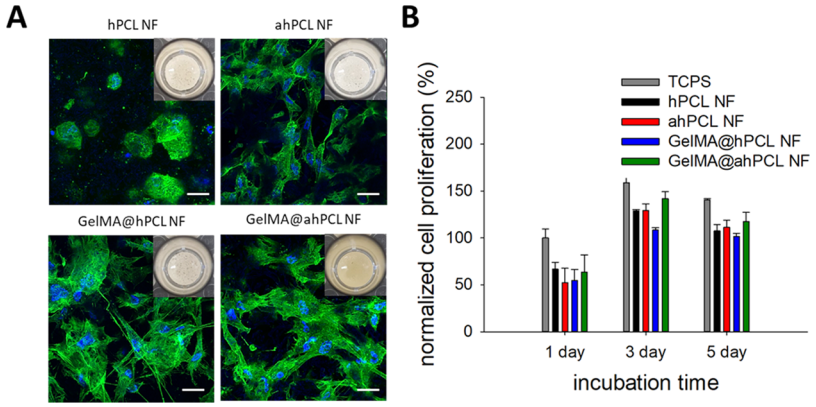

Figure 4. In vitro cultivation of HDF with various NFs and spontaneous formation of HDF/NF cell sheets. (A) CLSM of HDF/NF cell sheets at day 3. Z-stacked images (10 slices per sample, slice thickness = 4.1−6.9 μm) were superimposed to show 3D-associated HDF/NF cell sheets stained for nucleus (blue) and F-actin (green). Insets are digital photos of HDF/NF cell sheets in cell culture plates. (B) Cell proliferation of HDF in NF for 5 days based on the WST-1-based cell viability assay. The absorbance at 450 nm of all samples was normalized with respect to that of cells in TCPS at day 1.

performed better than physical coating. The morphology of these matrices was examined by scanning electron microscopy (SEM). Our results indicate that the length and diameter of the NFs did not change significantly after physical or chemical adsorption of GelMA, but the length of the NFs changed after aminolysis (Figure 2C). The length and diameter of hPCL NFs and GelMA@hPCL NFs were approximately 15 and 2 μm, respectively, and those of ahPCL NFs and GelMA@ahPCL NFs were 10 and 1.5 μm, respectively. A previous study indicated that electrospun PLA fibers fragmented in 1,6-hexanediamine/2-propanol became shorter over time due to fragmentation.[39] In another study, a PLA microfiber was chemically cut via aminolysis using different time periods and various ethylenediamine concentrations.[40] The results of that study indicated that extending the time of aminolysis progressively decreased the fiber length and increased the roughness of the fiber surface. These findings suggest that aminolysis likely decreases the fiber length and diameter via corrosive effects of ethylenediamine on polyesters.

We then analyzed the surfaces of the four types of NFs using X-ray photoelectron spectroscopy (XPS). Our results show that NFs decorated with GelMA showed unique peaks compared with those of native NFs not bearing GelMA (Figure 3). Wide-scan XPS showed that for all four NFs, C 1s and O 1s peaks appeared at 285.43 and 532.75 eV, respectively. For the two types of NFs coated with GelMA, the N 1s peak was observed at 400.14 eV, indicating that N was present on the corresponding NF. As verified by IVIS (Figure 2B), the N 1s peak of the chemically bonded GelMA@ahPCL NF showed a higher intensity over the same duration (Figure 3A). Deconvolution of high-resolution spectra for carbon elements in hPCL NF, ahPCL NF, GelMA@hPCL NF, and GelMA@ahPCL NF showed three subpeaks (Figure 3B). Furthermore, the following peaks were used to confirm and characterize the chemistry of GelMA decorated onto the surface of NFs: peak 1 near 284.6 eV, representing the carbon in C−C/C−H bonds; peak 2 near 287.88 eV, representing the carbon in C−O/C-N bonds; peak 3 near 288.68 eV,[40,41] representing the carbon in the C═O bond. As shown in a previous study, XPS peaks at approximately 286 eV, indicative of C−N and C−O bonding, do not appear clearly separated.[42] Similarly, peaks corresponding to C−O and C−N bonds appear at 285.5 and 286.2 eV, respectively, with nearly no difference in the binding energy.[43] XPS high-resolution spectra for C 1s were used to evaluate the ratio of peak areas of C−O/C−N bonds normalized to those of C−C/C−H (284.58 eV) (Figure 3C). Among the four NFs, GelMA@ahPCL NF showed the highest peak ratio for the carbon in C−O/C−N bonds normalized to the peak indicating the carbon in C−C/C−H bonds. This suggests that GelMA@ahPCL NF contained the highest number of C−N bonds among the four NFs. In summary, XPS analysis of surface chemistry showed that the area of C−O/C−N bonds was altered by chemical treatment and that GelMA@ahPCL NFs adsorbed the highest amount of GelMA among the four NFs.

To investigate the effect of GelMA immobilization on the surface of the NFs, we cultured HDF cells in the presence of respective NFs in non-treated 48-well plates. After 24 hours of culture, cell sheets composed of HDF and NFs started to form for all of the NF groups. However, cell sheet self-assembly of NFs containing gelatin or GelMA occurred more rapidly than that of non-decorated NFs; on day 3, the cell sheet containing GelMA@ahPCL NFs showed the most condensed association of cell−matrix complexes compared with those of other groups (Figure 4A, insets). Furthermore, cells in GelMA-associated NF (GelMA@hPCL NF, GelMA@ahPCL NF) exhibited more spread shapes in comparison to non-decorated NF (hPCL NF, ahPCL NF). Similarly, we previously observed that hPCL NFs self-assembled into cell sheets when cells were cultured with this matrix in untreated cell culture plates.[19] We speculate that immobilized gelatin can facilitate interactions between cells and NF because gelatin exerts high proliferation. Confocal laser scanning microscopy (CLSM) revealed that cells on NFs containing gelatin showed a higher degree of proliferation and spreading compared with cells grown on non-decorated counterparts. Cells cultured with hPCL NFs were round on day 3, while cells cultured with GelMA@hPCL NFs and GelMA@ahPCL showed a stretched morphology with enhanced expression of cytoskeletal proteins. Previously, we revealed that PCL NFs, produced by electrospinning, provided an artificial environment that closely resembled ECM microstructures in native tissues; in this artificial environment, a cell sheet was formed via interactions between HDF cells and NFs within 24 h. Three-dimensional sheet structures have been obtained via spontaneous assembly when gelatin and GelMA were added to hPCL NFs and cocultured with HDF cells.[30]

DOI: 10.1021/acsomega.9b02602
ACS Omega 2019, 4, 18677−18684

Similarly, the cores of GelMA@ahPCL NFs and PCL NFs can serve as adhesion points for anchorage-dependent cells, while decorated gelatin moieties can enhance the viability of the attached cells by providing denatured components of natural ECM. Gelatin-based scaffolds can promote cell adhesion[44] and have similar properties to those of ECM[45] due to the presence of a matrix metalloproteinase-responsive peptide motif that induces cell proliferation and spreading. Thus, we quantified the proliferation of HDF cells in the cell sheets over the course of 5 days (Figure 4B). When rates of cell proliferation were normalized with respect to the number of cells present on TCPS on day 1, we found that levels of proliferation had gradually increased according to the degree of gelatin decoration. On day 1, the four types of sheets showed similar levels of proliferation. However, on day 3, cell proliferation on GelMA@ahPCL NFs was higher than that on other NFs. These differences were statistically significant. Although GelMA@hPCL NFs and GelMA@ahPCL NFs generated similar cell spreading behaviors, the level of cell proliferation on GelMA@ahPCL NFs was higher than that on GelMA@hPCL NFs. This can be contributed to the degree of gelatin decoration on the NFs. Figures 2B and 3C confirmed higher levels of gelatin decoration in GelMA@ahPCL NFs compared with those of GelMA@hPCL NFs. Thus, GelMA@ahPCL NFs can be used as a scaffold for 3D cell culture, while decorated GelMA can enhance the proliferation of the attached cells, resulting in an increased cellular viability (Figure 4B). However, no further proliferation was observed on day 5 because our cell sheet had a confined area, which limited the space available for cell growth. The WST-1 assay can reflect the metabolic status of individual cells; however, more importantly, the higher the cell number, the higher the WST-1 absorbance measured. Thus, in terms of determining proliferation levels, we normalized WST-1 values with respect to those at day 1 to monitor the increase of cell numbers. Additionally, aminolysis of NF did not affect the biocompatibility of the matrix becasuse ahPCL NF and hPCL NF did not show a dramatic difference of the viability.

CONCLUSIONS

Michael-type addition between vinyl groups of GelMA and surface-exposed amines of ahPCL NFs resulted in a higher degree of decoration on ahPCL NFs compared with that on hPCL NFs. GelMA@ahPCL NFs markedly facilitated cell sheet formation, and HDF cells showed higher levels of viability and cell spreading in the cell sheets compared with those on GelMA@hPCL NFs or NFs not containing gelatin. Therefore, a simple strategy of gelatin decoration on NF can be a promising method to engineer surfaces of the fibrous matrix to enhance 3D construction of the cell/matrix complex.

EXPERIMENTAL SECTION

Materials. Poly(caprolactone) (PCL, MW 43,000) was purchased from Polysciences (Warrington, PA). Gelatin type A was purchased from MP Biomedicals (Illkirch, France). Ethylenediamine was purchased from Junsei (Kyoto, Japan). Fluorescamine, fluorescein isothiocyanate isomer I, 4′,6-diamidino-2-phenylindole dihydrochloride (DAPI), and methacrylic anhydride were purchased from Sigma-Aldrich (St. Louis, MO). Human dermal fibroblasts (HDFs), low serum growth supplement (LSGS), and bicinchoninic acid (BCA) protein assay kit were purchased from ThermoFisher Scientific, Inc. (Rockford, IL). Formaldehyde was purchased from Wako Chemicals (Osaka, Japan). Dulbecco's phosphate-buffered saline (PBS), Dulbecco's modified Eagle's medium (DMEM), streptomycin/penicillin, trypsin/EDTA, fetal bovine serum, and Alexa Fluor 488 phalloidin were purchased from Invitrogen (Carlsbad, CA). Water-soluble tetrazolium salt (WST-1) was purchased from DAEIL Lab (Seoul, Republic of Korea).

Electrospinning. PCL nanofibers were fabricated via partial digestion of electrospun PCL nanofibers as described in our previous study.[19] Briefly, 25% (w/v) solution of PCL in a chloroform/methanol mixture (3:1, v/v) was electrospun at 15 kV using a flow rate of 1 mL/h through a 25-G needle. Electrospun nanofibers were fabricated at temperature ranging 20−25 °C and relative humidity ranging 16−20%. The electrospun nanofiber was collected onto the aluminum foil ground for 10 min at a ground-to-needle distance of 15 cm. The PCL nanofibers were detached with ethanol and milled for 30 s; this step was repeated 3 times.

Fabrication of NFs. Milled nanofibers were hydrolyzed in 1.0 M solution of sodium hydroxide at 37 °C for 12 h. hPCL NFs were filtered through a sieve having 100 μm pore size, then washed with distilled water, and pelleted via centrifugation 3 times. Consequently, hPCL NFs (300 mg) were aminolyzed in 60 mL of 1.0 M ethylenediamine/methanol at 37 °C with magnetic stirring for 72 h. ahPCL NFs were washed 4 times with methanol, once with distilled water, and then freeze-dried. The surface-exposed primary amine groups on hPCL or ahPCL NFs were quantified using a fluorescamine assay as described previously.[46] Briefly, 1 mg of NFs was placed into 1 mL of methanol; this solution was then combined with 0.3 mg/mL fluorescamine in 0.1 mL of acetone. The mixture was stirred vigorously and incubated at room temperature in the dark for 30 min. Afterward, NFs were washed with methanol and redissolved in 1 mL of 1,4-dioxane. The fluorescence intensity was measured at Ex 390/Em 475 nm using a spectrofluorophotometer (Shimadzu Corporation, Japan). Ethylenediamine was used as a standard.

Gelatin Immobilization on NFs. To immobilize gelatin, NFs were chemically reacted with GelMA via Michael-type addition. Briefly, 0.2 mL of methacrylic anhydride (MA) was slowly added to a 10% (w/v) gelatin solution (10 mL) under vigorous stirring and the mixture was reacted at 50 °C for 3 h to obtain GelMA. The resulting solution was precipitated thrice in ice-cold ethanol to remove unreacted MA, and the precipitated GelMA was freeze-dried. Methacrylation of gelatin in D_2O was confirmed using ^1H NMR spectroscopy at the Central Laboratory of Kangwon National University (JNM-ECZ400S/L1, Japan). NFs (20 mg) were incubated with GelMA dissolved in PBS (30 μg/mL, 10 mL, pH 7.4) under magnetic stirring at 37 °C for 1−12 h. The degree of GelMA immobilization was determined via BCA assay as described previously. Briefly, NFs immobilized onto GelMA were washed 3 times using 0.1% (w/v) Tween-20; this step was used to physically disassociate GelMA and NFs, thereby removing GelMA from NFs. All NFs were freeze-dried overnight before the analysis. The amount of conjugated proteins on the NFs was evaluated via the BCA-based assay according to the manufacturer's instructions. Briefly, 0.1 mg of NFs was dissolved in 0.1 mL of boiled distilled water. Then, a BCA-based working reagent (0.1 mL) was added to samples (0.1 mg) and incubated at 37 °C for 30 min. The absorbance was

DOI: 10.1021/acsomega.9b02602
ACS Omega 2019, 4, 18677−18684

measured at 562 nm using Multiskan GO (Thermo Scientific, UK). Native GelMA was used as a standard.

Characterization of GelMA-Conjugated NFs. NFs dispersed in ethanol were placed on aluminum foil, and samples were observed by field-emission resolution scanning electronic microscopy (FE-SEM) (S-4300; Hitachi, Tokyo, Japan) at the Central Laboratory of Kangwon National University. For visualization, GelMA-conjugated NFs were incubated with fluorescein isothiocyanate isomer I-labeled GelMA (FITC-GelMA) and evaluated using an in vivo imaging system (IVIS 2000; PerkinElmer, Waltham, MA) at the Korea Basic Science Institute. Immobilization of GelMA on NFs was determined by X-ray photoelectron spectroscopy (XPS) (Thermo Scientific, UK) at the Central Laboratory of Kangwon National University, and spectra were obtained for C 1s, N 1s, and O 1s. High-resolution scans were obtained for carbon (C 1s).

Fabrication of NF/Cell Sheet. A suspension of HDF cells at passage 5 (2×10^5 cells/well) in DMEM was thoroughly mixed with 2 mg of hPCL NF, GelMA@hPCL NF, ahPCL NF, or GelMA@ahPCL NF via gentle pipetting, and the mixture (400 μl) was seeded into an untreated 48-well plate containing DMEM supplemented with low serum growth supplement (LSGS) and 1% (v/v) streptomycin/penicillin. The matrix/cell complexes were cultured at 37 °C and 5% CO_2. The cell culture medium was replaced daily. Cell proliferation was determined using a WST-1-based colorimetric assay according to the manufacturer's instructions. Briefly, 20 μl of WST-1 solution was added to each well of the 48-well plate described above and incubated at 37 °C for 30 min. The absorbance was measured at 450 nm via Multiscan GO (Thermo Scientific, UK). To evaluate the effect of hPCL NFs, GelMA@hPCL NFs, ahPCL NFs, and GelMA@ahPCL NFs on cell proliferation and spreading, the NF/cell complexes were fixed with 3.7% formaldehyde solution for 50 min and treated with Triton X-100 (0.1%, v/v) for 5 min. The samples were stained with Alexa Fluor 488 phalloidin for 50 min and counterstained with DAPI for 3 min for F-actin and nucleus visualization, respectively. The NF/cell complexes were evaluated via confocal laser scanning microscopy (CLSM) using a diode laser at 405 nm for DAPI and a Mar laser at 488 nm for Alexa Flour and 488 phalloidin at the Central Laboratory of Kangwon National University.

■ ASSOCIATED CONTENT

Supporting Information

The Supporting Information is available free of charge on the ACS Publications website at DOI: 10.1021/acsomega.9b02602.

3D reconstruction of confocal microscopic images of HDF (Figure S1) (PDF)

■ AUTHOR INFORMATION

Corresponding Author

*E-mail hsyoo@kangwon.ac.kr.

ORCID

Hyuk Sang Yoo: 0000-0002-4346-9154

Notes

The authors declare no competing financial interest.

■ ACKNOWLEDGMENTS

This work was supported by the National Research Foundation of Korea (NRF-2019R1I1A2A01040849).

■ REFERENCES

(1) Yang, J.; Yamato, M.; Kohno, C.; Nishimoto, A.; Sekine, H.; Fukai, F.; Okano, T. Cell sheet engineering: recreating tissues without biodegradable scaffolds. *Biomaterials* **2005**, *26*, 6415−6422.

(2) Edmondson, R.; Broglie, J. J.; Adcock, A. F.; Yang, L. Three-dimensional cell culture systems and their applications in drug discovery and cell-based biosensors, Assay and Drug development technologies. *Assay Drug Dev. Technol.* **2014**, *12*, 207−218.

(3) Owaki, T.; Shimizu, T.; Yamato, M.; Okano, T. Cell sheet engineering for regenerative medicine: current challenges and strategies. *Biotechnol. J.* **2014**, *9*, 904−914.

(4) Kook, Y. M.; Jeong, Y.; Lee, K.; Koh, W. G. Design of biomimetic cellular scaffolds for co-culture system and their application. *J. Tissue Eng.* **2017**, *8*, 1−17.

(5) Duval, K.; Grover, H.; Han, L. H.; Mou, M.; Pegoraro, A. F.; Fredberg, J.; Chen, Z. Modeling Physiological Events in 2D vs. 3D Cell Culture. *Physiology* **2017**, *32*, 266−277.

(6) Greene, T.; Lin, T. Y.; Andrisani, O. M.; Lin, C. C. Comparative study of visible light polymerized gelatin hydrogels for 3D culture of hepatic progenitor cells. *J. Appl. Polym. Sci.* **2017**, *134*, No. 44585.

(7) Ozawa, F.; Ino, K.; Shiku, H.; Matsue, T. Cell sheet fabrication using RGD peptide-coupled alginate hydrogel fabricated by an electrodeposition method. *Chem. Lett.* **2017**, *46*, 605−608.

(8) Kessler, L.; Gehrke, S.; Winnefeld, M.; Huber, B.; Hoch, E.; Walter, T.; Wyrwa, R.; Schnabelrauch, M.; Schmidt, M.; Kuckelhaus, M.; Lehnhardt, M.; Hirsch, T.; Jacobsen, F. Methacrylated gelatin/hyaluronan-based hydrogels for soft tissue engineering. *J. Tissue Eng.* **2017**, *8*, 1−14.

(9) Sharif, S.; Ai, J.; Azami, M.; Verdi, J.; Atlasi, M. A.; Shirian, S.; Samadikuchaksaraei, A. Collagen-coated nano-electrospun PCL seeded with human endometrial stem cells for skin tissue engineering applications. *J. Biomed. Mater. Res., Part B* **2018**, *106*, 1578−1586.

(10) Ren, Z.; Ma, S.; Jin, L.; Liu, Z.; Liu, D.; Zhang, X.; Cai, Q.; Yang, X. Repairing a bone defect with a three-dimensional cellular construct composed of a multi-layered cell sheet on electrospun mesh. *Biofabrication* **2017**, *9*, No. 025036.

(11) Yang, X.; Shah, J. D.; Wang, H. Nanofiber enabeled layer-by-layer approach toward three-dimensional tissue formation. *Tissue Eng., Part A* **2009**, *15*, 945−956.

(12) Asencio, I. O.; Mittar, S.; Sherborne, C.; Raza, A.; Claeyssens, F.; MacNeil, S. A methodology for the production of microfabricated electrospun membranes for the creation of new skin regeneration models. *J. Tissue Eng.* **2018**, *9*, 1−8.

(13) Kim, Y. J.; Matsunaga, Y. T. Thermo-responsive polymers and their application as smart biomaterials. *J. Mater. Chem. B* **2017**, *5*, 4307−4321.

(14) Lee, Y. B.; Shin, Y. M.; Kim, E. M.; Lee, J. Y.; Lim, J. S.; Kwon, S. K.; Shin, H. S. Mussel adhesive protein inspired coatings on temperature-responsive hydrogels for cell sheet engineering. *J. Mater. Chem. B* **2016**, *4*, 6012−6022.

(15) Smith, M. J.; Smith, D. C.; White, K. L.; Bowlin, G. L. Immune response testing of electrospun polymers: An important consideration in the evaluation of biomaterials. *J. Eng. Fibers Fabr.* **2007**, *2*, 41−47.

(16) Lu, W.; Sun, J.; Jiang, X. Recent advances in electrospinning technology and biomedical applications of electrospun fibers. *J. Mater. Chem. B* **2014**, *2*, 2369−2380.

(17) Madani, M.; Sharifi-SanjaniAhma, N.; Hasan-Kaviar, A.; Choghazardi, M.; Hamouda, A. S. PS/TiO2 (polystyrene/titanium dioxide) composite nanofibers with higher surface-to-volume ratio prepared by electrospinning: morphology and thermal properties. *Polym. Eng. Sci.* **2012**, *53*, 2407−2412.

(18) Han, N.; Johnson, F. K.; Bradley, P. A.; Parikh, K. S.; Lannutti, J. J.; Winter, J. O. Cell attachment to hydrogel-electrospun fiber mat composite materials. *J. Funct. Biomater.* **2012**, *3*, 497−513.

DOI: 10.1021/acsomega.9b02602
ACS Omega 2019, 4, 18677−18684

(19) Lee, S.; Kim, H. S.; Yoo, H. S. Electrospun NFs embedded hydrogel composites for cell cultivation in a biomimetic environment. *RSC Adv.* **2017**, *7*, 54246−54253.
(20) Son, Y. J.; Kim, H. S.; Mao, W.; Park, J. B.; Lee, D.; Lee, H.; Yoo, H. S. Hydro-nanofibrous mesh deep cell penetration: a strategy based on peeling of electrospun coaxial nanofibers. *Nanoscale* **2018**, *10*, 6051−6059.
(21) Wu, J.; Hong, Y. Enhancing cell infiltration of electrospun fibrous scaffolds in tissue regeneration. *Bioact. Mater.* **2016**, *1*, 56−64.
(22) Kim, H. S.; Yoo, H. S. Surface-polymerized biomimetic NFs for the cell-directed association of 3-D scaffolds. *Chem. Commun.* **2015**, *51*, 306−309.
(23) Azimi, B.; Nourpanah, P.; Rabiee, M.; Arbab, S. Poly (ε-caprolactone) fiber: an overview. *J. Eng. Fibers Fabr.* **2014**, *9*, 74−90.
(24) Malikmammadov, E.; Tanir, T. E.; Kiziltay, A.; Hasirci, V.; Hasirci, N. PCL and PCL-based materials in biomedical applications. *J. Biomater. Sci.* **2018**, *29*, 863−893.
(25) Kai, D.; Liow, S. S.; Loh, X. J. Biodegradable polymers for electrospinning: Towards biomedical applications. *Mater. Sci. Eng.: C* **2014**, *45*, 659−670.
(26) Son, Y. J.; Kim, H. S.; Yoo, H. S. Layer-by-layer surface decoration of electrospun nanofibrous meshes for air-liquid interface cultivation of epidermal cells. *RSC Adv.* **2016**, *6*, 114061−114068.
(27) Monnier, A.; Tawil, E. A.; Nguyen, Q. T.; Valleton, J.-M.; Fatyeyeva, K.; Deschrevel, B. Functionalization of poly(lactic acid) scaffold surface by aminolysis and hyaluronan immobiliztion: how it affects mesenchymal stem cell proliferation. *Eur. Polym. J.* **2018**, *107*, 202−217.
(28) Benesch, R.; Benesch, R. E. Formation of peptide bonds by aminolysis of homocysteine thiolactones. *J. Am. Chem. Soc.* **1956**, *78*, 1597−1599.
(29) Costantini, M.; Testa, S.; Fornetti, E.; Barbeta, A.; Trombetta, M.; Cannata, S. M.; Gargioli, C.; Rainer, A. Engineering muscle networks in 3D GelMA hydrogels: influence of mechanical stiffness and geometrical confinement. *Front. Bioeng. Biotechnol.* **2017**, *5*, No. 22.
(30) Mao, W.; Kang, M. K.; Shin, J. U.; Son, Y. J.; Kim, H. S.; Yoo, H. S. Coaxial hydro-nanofibirls for self-assembly of cell sheets producing skin bilayers. *ACS Appl. Mater. Interfaces* **2018**, *10*, 43503−43511.
(31) Zhang, Z.; Loebus, A.; Vicente, G. D.; Ren, F.; Arafeh, M.; Ouyang, Z.; Lensen, M. C. Synthesis of poly(ethylene glycol)-based hydrogels via amine-michael type addition with tunable stiffness and polstelation chemical functionality. *Chem. Mater.* **2014**, *26*, 3624−3630.
(32) Khunmanee, S.; Jeong, Y.; Park, H. Crosslinking method of hyaluronic-based hydrogel for biomedical applications. *J. Tissue Eng.* **2017**, *8*, 1−16.
(33) Russell, R. J.; Sirkar, K.; Pishko, M. V. Preparation of Nanocomposite poly(allylamine)-poly(ethylene glycol) thin films using michael addition. *Langmuir* **2000**, *16*, 4052−4054.
(34) Weissman, M. R.; Winger, K. T.; Ghiassian, S.; Gobbo, P.; Workentin, M. S. Insights on the Application of the Retro Michael-Type Addition on Maleimide-Functionalized Gold Nanoparticles in Biology and Nanomedicine. *Bioconjugate Chem.* **2016**, *27*, 586−593.
(35) Vernon, B.; Tirelli, N.; Bachi, T.; Haldimann, D.; Hubbell, J. A. Water-borne, in situ crosslinked biomaterials from phase-segregated precursors. *J. Biomed. Mater. Res., Part A* **2003**, *64A*, 447−456.
(36) Lin, C. C.; Anseth, K. S. PEG hydrogels for the controlled release of biomolecules in regenerative medicine. *Pharm. Res.* **2009**, *26*, 631−643.
(37) Bakry, A.; Darwish, M. S. A.; El Naggar, A. M. A. Assembling of hydrophilic and cytocompativle three-dimensional scaffolds based on aminolyzed poly (L-lactide) single crystals. *New J. Chem.* **2018**, *42*, 16930−16939.
(38) Zhu, Yabin.; Gao, Changyou.; Liu, Xingyu.; Shen, Jiacong. Surface modification of polycaprolactone membrane via aminolysis and biomacromolecule immobilization for promting cytocompatibility of human endothelial cells. *Biomacromolecules* **2002**, *3*, 1312−1319.
(39) Thiré, R. M.S.M.; O.Meiga, Taila.; Dick, Sabrina.; Leonardo, R. Andrade. Functionalization of biodegradable polyester for tissue engineering applications. *Macromol. Symp.* **2007**, *258*, 38−44.
(40) Petre, D.-G.; Kuckoa, N. W.; Abbadessa, A.; Vermonden, T.; Polini, A.; Leeuwenburgh, S. C. G. Surface functionalization of polylactic acid fibers with alendronate groups does not improve the mechanical properties of fiber-reinforced calcium phosphate cements. *J. Mech. Behav. Biomed. Mater.* **2018**, *90*, 472−483.
(41) Rodrigues, A. F.; Newman, L.; Lozano, N.; Mukherjee, S. P.; Fadeel, B.; Bussy, C.; Korstarelos, K. A blueprint for the synthesis and characterization of thin graphene oxide with controlled lateral dimensions for biomedicine. *2D Mater.* **2018**, *5*, No. 035020.
(42) Zhang, B.; Lin, Z.; Huang, J.; Cao, L.; Wu, X.; Yu, X.; Xie, Y. Z. F.; Zhang, W.; Chen, J.; Mai, W.; Xie, W.; Meng, H.; et al. Highly active and stable non noble metal catalyst for oxygen reduction reaction. *Int. J. Hydrogen Energy* **2017**, *42*, 10423−10434.
(43) Yuan, S.; Xiong, G.; Roguin, A.; Teoh, S. H.; Choong, C. Amelioration of blood compatibility and endothelialization of polycaprolactone substrates by surface-initiated atom transfer radical polymerization. *Adv. Biomater. Sci. Biomed. Appl.* 2013, DOI: DOI: 10.5772/52646.
(44) Liu, Y.; Park, M. B. C. A biomimetic hydrogel based on methacrylated dextran-*graft*-lysin and gelatin for 3D smooth muscle cell culture. *Biomaterials* **2010**, *31*, 1158−1170.
(45) Yue, K.; Santiago, G. T.; Alvarez, M. M.; Tamayol, A.; Annabi, N.; Khademhosseini, A. Synthesis, properties, and biomedical applications of gelatin methacryloyl (GelMA) hydrogels. *Biomaterials* **2015**, *73*, 254−271.
(46) Son, Y. J.; Kang, J. H.; Kim, H. S.; Yoo, H. S. Electrospun nanofibrous sheets for selective cell capturing in continuous flow in microchannels. *Biomacromolecules* **2016**, *17*, 1067−1074.

DOI: 10.1021/acsomega.9b02602
ACS Omega 2019, 4, 18677−18684